



Deep-hole directional fracturing of thick hard roof for rockburst prevention

Hu He^{a,b}, Linming Dou^{b,*}, Jun Fan^b, Taotao Du^c, Xinglin Sun^b

^a School of Resource and Earth Science, China University of Mining and Technology, Xuzhou, Jiangsu 221008, PR China

^b State Key Laboratory of Coal Resources and Safe Mining, China University of Mining and Technology, Xuzhou, Jiangsu 221008, PR China

^c Beijing Mining Research Institute, China Coal Research Institute, Beijing 100013, PR China

ARTICLE INFO

Article history:

Received 5 January 2012

Received in revised form 16 April 2012

Accepted 1 May 2012

Available online 2 June 2012

Keywords:

Directional fracturing

Rockburst

Hard roof

Initial groove

Microseismic

ABSTRACT

Thick hard roof in coal mines is usually a significant factor that induces dynamic disasters, such as rockburst. This study introduces a new technology called directional hydraulic fracturing characterized by cutting out an initial groove in the borehole and then injecting high pressure liquid to break the rock. The abutment pressure on the groove tip and fracture criterion is worked out based on the fracture mechanics taking fluid seepage into consideration. Computational simulations revealed that the vertical compressive stress changed to tension immediately after high pressure liquid injected into the fracturing hole, the concentration factor up to 5 that can easily rupture the roof and reduce the rockburst hazard at the same time. The seamless steel tubes are used instead of high pressure hose and conveyed into fracturing holes by geological drill to the designed locations, so as to break through the depth limitation and make the whole process automated. In situ applications at two longwall faces of LW6305 and LW5307 show that the depth can easily reach to 20 m and the fracture radius more than 13 m within half an hour, the efficiency and security are greatly improved. We can determine whether the roof is split by observing the pressure changes. The pressure of liquid during fracturing process can be divided into three stages: dramatically ascending, descending and stable, corresponding to crack initiation, propagation and dissemination, respectively. Drilling bits method and microseismic system validate prevention effects of this technique notably so that lead to a foundation for large scale popularization and application in China coal mine.

© 2012 Elsevier Ltd. All rights reserved.

1. Introduction

As we all know that China has been the largest coal production country, but China is also the most severe mining areas suffered from the dynamic disasters of rockburst or coal bump, accounted for one third of the total in the world (Li et al., 2007; Dou et al., 2009). In the past few decades rockburst disasters occurred in more than 100 collieries caused numerous injuries, fatal accidents and property loss. But majority of people engaged in coal industry had little knowledge on this dynamic phenomenon, so rockburst is always a research hotspot and difficulty of rock mechanics (Dou et al., 2006). Researchers at home and abroad carried out studies mainly focused on three aspects that mechanism, prediction and control methods. Great achievements had been obtained especially the breakthrough work of Cook that gave us better understandings on the essential process of rockburst (Cook, 1965). Afterwards many theoretical and numerical models have been developed in mechanism analysis (Salamon, 1984; Gibowicz and Kijko, 1994; Fujii et al., 1997; Dou and He, 2001; Blake and Hedley, 2001; Sharan,

2007; Zhu et al., 2010; He et al., 2010). However, in the mining field the engineers most concerns about how to control and eliminate the hazards efficiently and safely since no monitoring method has proven entirely reliable for dangerous degree prediction though a variety of countermeasures are used (Salamon, 1984; Brady and Rowell, 1986; Srinivasan et al., 1997; Mansurov, 2001).

The prevention methods of rockburst can be classified into two categories: long-term strategy and instant destress. Long-term strategy includes layout of workforce and coal seam exploitation sequence, but the mining system can be hardly changed once formed, so during the coal mining destress must be carried out aiming to the dangerous areas. Hard thick roof is usually the main factor that causes excessive stress concentration and induces dynamic strata behaviors. Theoretical analysis and in situ seismic monitoring results indicate that most sources of rockburst are located in strata with high strength and integrity especially thick sandstone immediately overlying the seam, so hard thick sandstone roof is treated as the sign of rockburst in many countries (Dou et al., 2006). Blasting and water injection are traditionally used to control the hard roof, however these two means have obviously inherent defects, for example, blasting can only be utilized in low gas mines and misfire is very hard to tackle, as for water injection, the effect will be whittled down greatly due to high compactness and low permeability

* Corresponding author. Tel.: +86 13705206814; fax: +86 051683995904.

E-mail address: hehu_cumt@126.com (L. Dou).

Nomenclature

σ_1, σ_3	the maximum and minimum principal stress in the rock mass (MPa)	R_t	the tensile strength of the hard roof (MPa)
$\sigma_x, \sigma_y, \tau_{xy}$	normal and shear stress components acted on the groove (MPa)	μ	the dynamic viscosity of the high pressure liquid (Pa s)
β	the angle between σ_1 and σ_y ($^\circ$)	l	the crack length (m)
σ_b	the tangential stress at any point on the groove (MPa)	\bar{V}	the liquid velocity (m/s)
m	the axis ratio of the ellipse	k	the permeability of liquid in the hard roof ($\mu\text{m}^2 \times 10^{-6}$)
α	the eccentric angle between the line from a point to the center with the X-axis ($^\circ$)	P'	the pore pressure (MPa)

(Dubinski, 1994; Board et al., 1992; Tang, 2000; Klishin, 2006). New technology that much more effective than traditional methods with little risk must be developed with the increasing requirements of safety. In this study the application of deep-hole directional hydraulic fracturing at Jining No. 3 coal mine in Shandong province is presented, series of difficulties and key parameters are solved to make this technique practical and can take the place of blasting in the near future.

2. Method of directional fracturing of hard roof

The hydraulic fracturing technology has been researched both in China and abroad, great achievements have been obtained after decades of development (Beach, 1980; Lenoach, 1995; Garcia and Sousa, 1997; Papanastasiou, 1997; Ruiting, 2006; Mofazzal and Rahman, 2008), but we found that most of the previous studies focused in the field of petrol exploitation and in situ stress measurements (Fairhurst, 1964; Haimson and Fairhurst, 1970; Ito et al., 1999; Rahman and Joarder, 2006). However applications of hydraulic fracturing in coal mine are just in its infancy currently, and mainly used to fracture the coal seam so as to increase permeability of gassy coal seams, improve hard thick top coal cavability and prevent coal and gas outbursts (Huang et al., 2007). Hydraulic fracturing of the coal seam is conducted by drilling a circle hole in the coal and then injecting liquid directly. Usually cracks can fissure with low hydraulic pressure since the coal seam is relatively soft compared with roof. If we plan to control hard thick main roof using hydraulic fracturing, the pressure of the liquid will be increased vastly and probably exceed the pump ability, moreover the propagation of the main cracks and airfoil branch fissures are determined by the stress field, so it is difficult to realize the directional slice of the roof.

The directional fracturing method is proposed by Polish experts of the Central Mining Institute mainly aiming to disintegrate the compact rocks, but few research papers that introduced the mechanism and technical parameters systematically have been reported

(Yan et al., 2000; Du et al., 2010). Fig. 1 shows that the essence of directional fracturing is the generation of a spatially oriented fracture in the rock mass and under the impact of high pressure liquid injected into the borehole, the cracks propagate from the tips of the oriented fracture thereby dividing the rock layers into blocks or plates with determined sizes and forms. Such a process is owing to the generation of the so-called initial groove with exactly spatial orientation in the borehole surroundings. This initial groove delimits the direction of fracture propagation and its rise is induced by the high pressure liquid. Both the integrity and strength of hard roof are weakened after fractured, as a result the sudden roof falling with large area is avoided and the rockburst danger reduced ultimately.

2.1. Mechanism of directional fracturing propagation

The crack of the initial groove under rock stress and liquid pressure is a typical category of fracture mechanics, so we establish a simplified plane model to analyze the stress distribution and the failure criterion around the initial groove, as shown in Fig. 2.

Based on the relationship of principal stress and the stress components around the ellipse fracture of elasticity theory, one can obtain the equations as follows:

$$\sigma_y = \frac{1}{2}(\sigma_1 + \sigma_3) - \frac{1}{2}(\sigma_1 - \sigma_3) \cos 2\beta, \quad \tau_{xy} = -\frac{1}{2}(\sigma_1 - \sigma_3) \sin 2\beta,$$

$$\sigma_x = \sigma_1 + \sigma_3 - \sigma_y \tag{1}$$

where σ_x, σ_y and τ_{xy} are the x and y-direction stresses component acted on the groove, respectively, σ_1 and σ_3 are the maximum and minimum principal stress, β is the angel between σ_1 and σ_y . The tangential stress σ_b at any point on the crack wall can be expressed by the Inglis equation (Wang et al., 2008) as:

$$\sigma_b = \{(\sigma_y - P_0)(m(m + 2)) \cos^2 \alpha + \sigma_x((1 + 2m) \sin^2 \alpha - m^2 \cos^2 \alpha) + \tau_{xy}(2(1 + m)^2 \sin \alpha \cos \alpha)\} / (m^2 \cos^2 \alpha + \sin^2 \alpha) \tag{2}$$

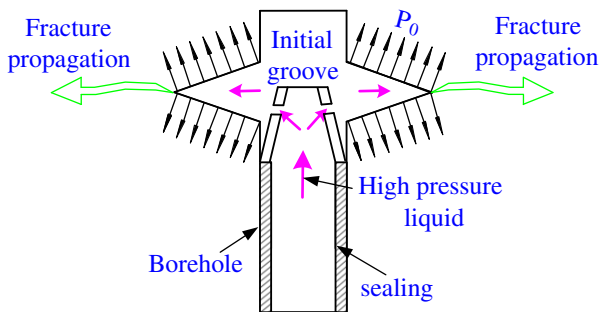


Fig. 1. Essence of directional fracturing.

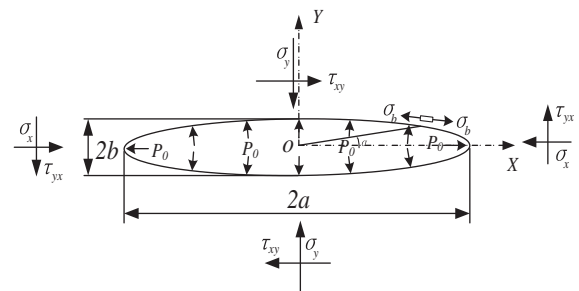


Fig. 2. Mechanical model of the artificial fracture in the hard roof.

where σ_b is the tangential stress of one point on the crack wall, P_0 is the pressure of hydraulic liquid, m is axis ratio of the ellipse that $m = a/b$, a is semi-major axis and b is semi-minor axis, α is eccentric angle with the X -axis. The failure of the initial fracture is attributed to σ_b which is the function of eccentric angle α , so the maximum of σ_b can be obtained by derivative of the angle. The tensile strength of rock mass is much smaller than the compressive or shear strength, so the crack tip is failed under tension stress, the maximum of σ_b and its location α are,

$$\sigma_{b\max} = \frac{(\sigma_1 - \sigma_3 - P_0)^2}{4m(\sigma_1 + \sigma_3 - P_0)},$$

$$\alpha = \frac{m\sqrt{(\sigma_1 - P_0 + 3\sigma_3)(3\sigma_1 - 3P_0 + \sigma_3)}}{\sigma_1 - P_0 - \sigma_3} \quad (3)$$

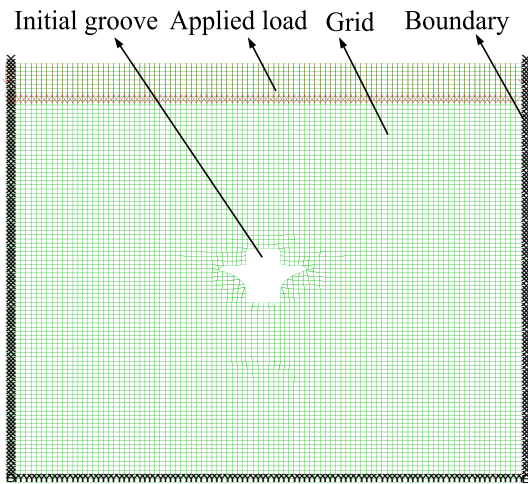


Fig. 3. Simulation model of the directional fracturing.

The Griffith fracture criterion (Atkinson, 1987) is adopted to determine the failure and propagation condition that when the tension stress exceeds the ultimate tensile strength the crack tip will fail and if the high pressure and flow liquid satisfy the Darcy law (Bear, 1972), the crack will propagate continually. So we can obtain the failure and propagation criterion and the required liquid pressure as:

$$\sigma_{b\max} \geq R_t + \mu l \bar{V} / k + P' \quad (4)$$

Using R stands for $R_t + \mu l \bar{V} / k + P'$, one can obtain:

$$P_0 \geq (\sigma_1 - \sigma_3) + 2mR + 2\sqrt{2mR(\sigma_3 + mR)} \quad (5)$$

where R_t is the tensile strength of hard roof rock mass, μ is the dynamic viscosity of the high pressure liquid, l is the crack length, \bar{V} is the liquid velocity, k is the permeability of liquid in the hard roof, and P' is pore pressure. The minimum pressure of hydraulic liquid can be assessed once we know about the in situ rock pressure, and of course in order to overcome the frictions and dissipation a standby coefficient must be taken into consideration.

2.2. Numerical simulation of stress distribution around the initial groove

Although the maximum tangential stress on the groove tip and the required liquid pressure are analyzed theoretically, the detailed stress distribution during the directional fracturing process is still unknown. Computational simulation is a good solution, two-dimensional explicit finite difference program FLAC 5.0 is used to analyze the stress distribution around the artificial initial groove in order to reveal the fracture mechanism. Fig. 3 shows the model grid, because the diameter of bore hole is just 42 mm, the model size cannot be too big, we build the model with 600 mm width and 700 mm height, divided into 10,000 grids averagely. The properties of the roof are as follows: density is 2540 kg/m³, cohesion is 3.5 MPa, angle of internal friction is 38°, shear and bulk modulus

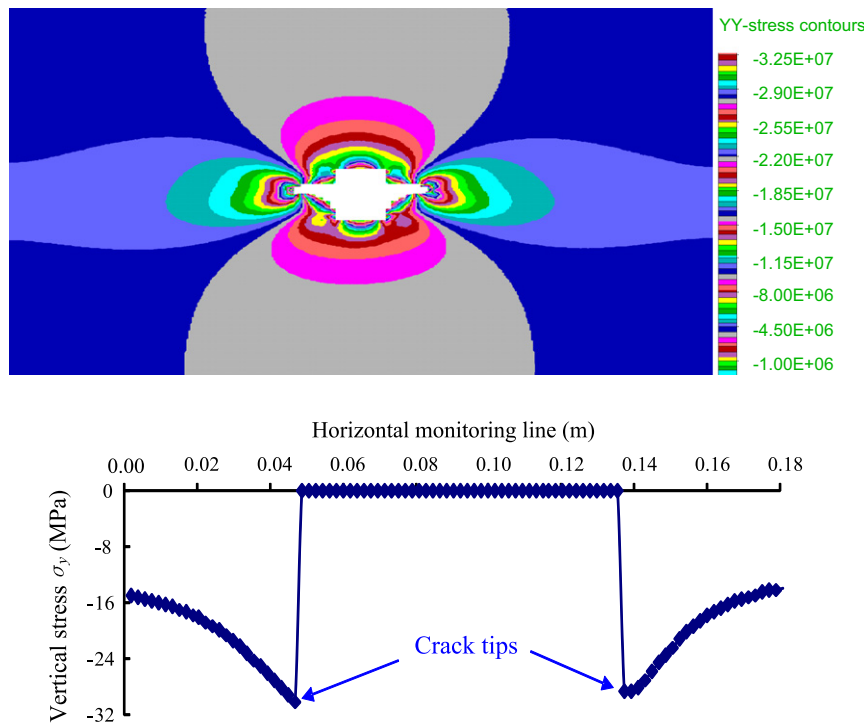


Fig. 4. Cloud picture of vertical stress distribution around initial groove before high pressure water injected.

are 16 GPa and 20 GPa, respectively. The constitutive behavior is elastic and simply supported is applied as the boundary conditions. Simulated burial depth is 400 m, so the initial stresses of σ_x , σ_y , σ_z are the same 10 MPa. After 10,000 steps, the calculation reaches to equilibrium.

Fig. 4 demonstrates that the vertical compressive stress concentrates around the artificial groove once cut out, and the maximum reaches 32 MPa that is about 3 times than the initial stress on the

tips. But the hard roof is still hardly broken because the stress did not exceed the strength limit. However Fig. 5 indicates that after the 30 MPa high pressure water injected into the bore hole the stress type changed to tension stress immediately and the maximum reaches to 50 MPa which surpasses most of the limits of roof rock in coal mines. As continuous injection of the high pressure water, the hard roof sustained damage and fracture, finally a crack plane is formed. By conducting out this technology at different

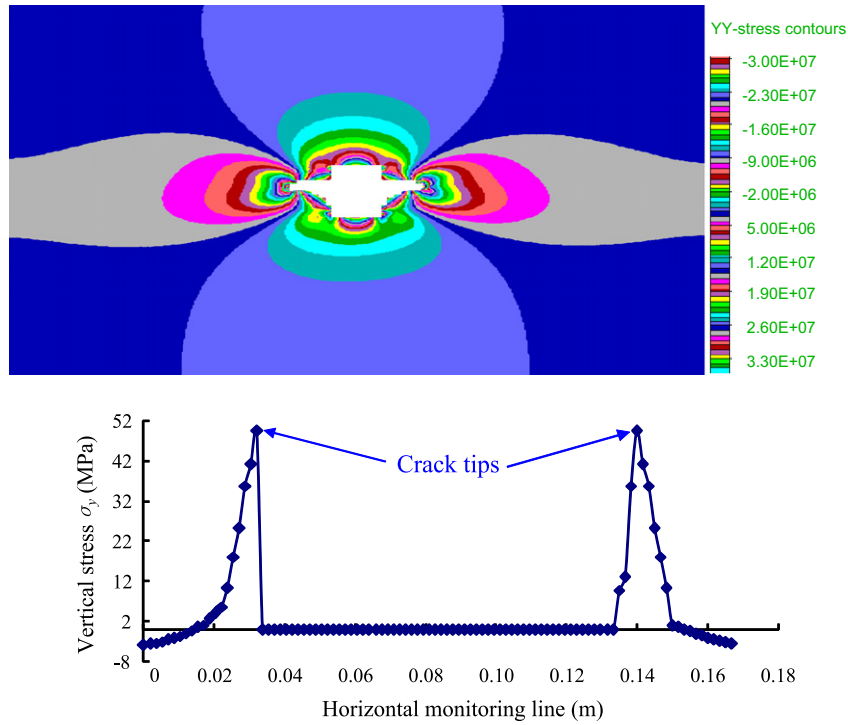
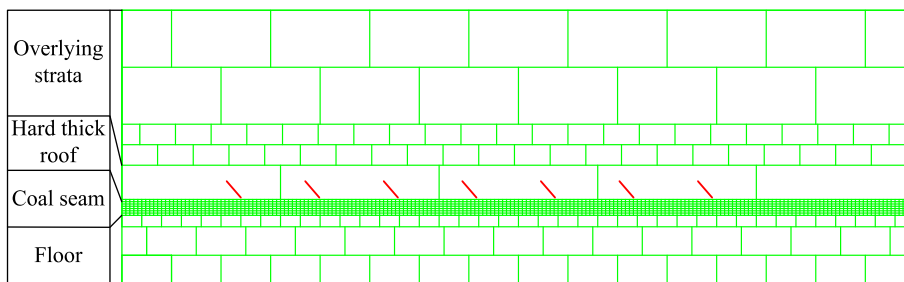
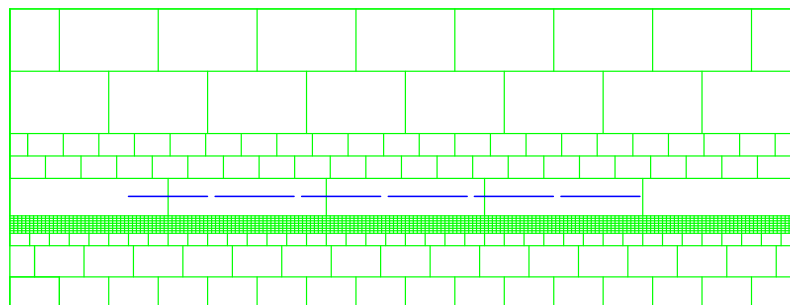


Fig. 5. Cloud picture of vertical stress distribution around initial groove after high pressure water injected.



(a) Hard roof treated by inclined directional fracturing



(b) Hard roof treated by horizontal directional fracturing

Fig. 6. UDEC numerical simulation model of hard roof directional fracture.

depth and place, the hard thick roof can be cut into several thin layers or short block, the caving interval sharply reduced, and the released elastic energy and dynamic impacts to the coal seam have weakened correspondingly, so the rockburst hazards induced by hard roof are eliminated effectively.

2.3. Numerical simulation of rockburst prevention by directional hydraulic fracturing

2.3.1. UDEC model of hydraulic fracturing of hard roof

A numerical calculation model was established with UDEC 3.1 (Universal Distinct Element Code) software which is a two-dimensional, discrete element numerical calculation program appropriate for non-continuum modeling. Its blocks can be rigid or deformed, and the contact must be deformed. UDEC solves the equations of motion and dynamic using a display difference method based on Lagrange which makes UDEC to have a unique advantage to simulate the crack and cave of the rock strata. Fig. 6 shows the UDEC model for simulation the reduction in rockburst potential after directional fracturing. Fig. 6a is inclined fracturing with 45° angle, and Fig. 6b is horizontal fracturing of the hard thick roof. The horizontal length and vertical height are 200 and 120 m, respectively, and the simulated mining depth is 650 m. Mechanical properties of the strata are given in Table 1.

The hard thick roof is divided into five blocks with 40 m length according to the field situation. The criterion of the Mohr–Coulomb’s model is adopted, and the boundary conditions are as follows: the transverse displacement and speed are zero at the left and right boundary while vertical displacement and speed is set to zero at the bottom boundary. Three schemes are simulated: (1) The hard thick main roof without any treatment; (2) the main roof treated with inclined fracturing; (3) the main roof sliced horizontally. The kinetic and total energy released from system which closely related to rockburst hazard are used as the index to demonstrate the change in rockburst potential before and after directional fracturing.

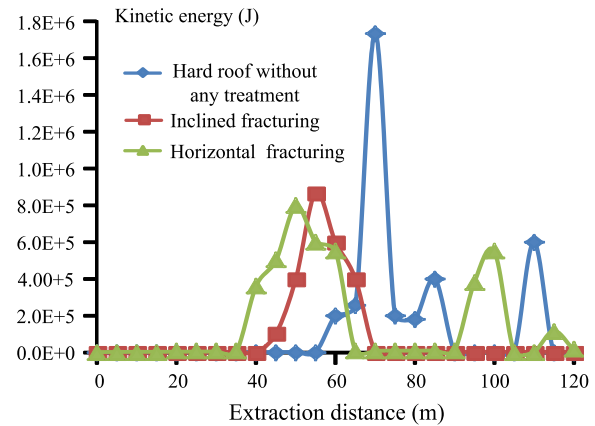
2.3.2. Analysis of rockburst hazard reduction after directional fracturing

Variation of the kinetic energy is shown in Fig. 7a. The maximum kinetic energy of the system was 1.68×10^6 J at the 65 m hanging roof before the hard roof cracked, after inclined and sliced fracturing the maximum kinetic energy severally declined to 8.39×10^5 and 8.16×10^5 J at 60 m and 50 m, respectively. It is manifest that more kinetic energy released, higher rockburst danger would be engendered.

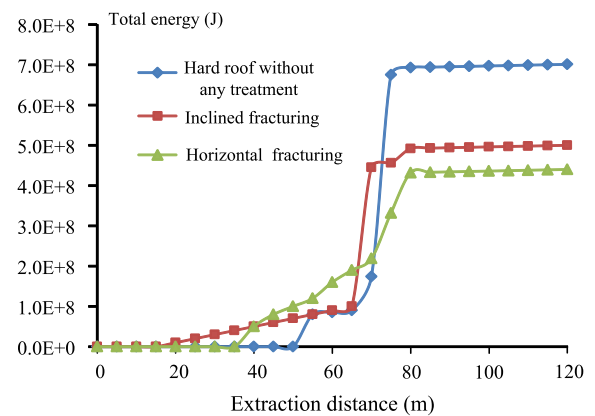
Fig. 7b demonstrates the variation of the total energy released during the coal exploitation. The released energy climbed gradually with the increase of excavation distance. Specifically, little energy was released before roof weighting but the energy level rose dramatically with the increasing length of hanging roof and finally reached equilibrium state. The total energy of the roof without any treatment is much more than the fractured roof. The least energy released is found in the horizontal fracturing situation and inclined

Table 1
Strata material properties.

Location	Lithology	Thickness (m)	Bulk modulus (GPa)	Shear modulus (GPa)	Density (kg/m ³)	Frictional angle (°)	Cohesion (MPa)	Tensile strength (MPa)
Roof	Fine sandstone	50	10	6	2600	33	15	10
Roof	Fine sandstone	18	10	4.5	2500	33	10	6
Main roof	Moderate coarse sandstone	15	9	4	2340	32	12	8
Coal seam	–	7	3.4	1.5	1340	30	1.5	1.5
Immediate floor	Siltstone	5	8	3	2500	28	18	8
Main floor	Sandstone	25	10	6	2600	33	20	10



(a) Kinetic energy released during the coal extraction



(b) Total energy released during the coal extraction

Fig. 7. Energy released during the coal extraction before and after hard roof fracturing.

fracturing took the second place. This suggests that the energy released from the system reduced greatly after main roof is fractured, and thus the danger of rockburst declined significantly.

As the thick hard roof is treated by directional fracturing, it can be seen that the integrity of main roof impaired, at the same time the length, thickness and weighting span of the thick hard roof reduced. As a result, kinetic and total energy released from system during the coal exploitation reduced remarkably, thereby achieving the aim of preventing rockburst hazard.

3. Field test and application

3.1. Introduction of the coal mine

The field experiments and application were carried out at two 660 m deep longwall workfaces, LW6305 and LW5307 in Jining

No. 3 coal mine located in Shandong Province, eastern China. The coal seam is 6.5 m thick averagely adopting fully mechanized sub-level caving method for coal mining. The sandstone main roof is 16.77–41.12 m average 28 m thick with a tensile strength of 8–10 MPa, and immediately lay above on the coal seam. During the coal extraction, mining tremors and rockburst occurred frequently dominantly due to the caving of thick hard main roof with a hanging length over 50 m. So pre-weaken to the roof is the essential method in order to eliminate the rockburst hazards.

3.2. On-site process

3.2.1. Layout of fracturing drilling holes

LW6305 is 240 m wide and 860 m in length, the experiment area is near the terminal line where the underground pressure is much higher than other regions because of the big protective pillar for the main roadways. The aim of the directional fracturing at LW6305 is prevention the potential rockburst near the terminal line. Fig. 8 shows the planar and profile of boreholes layout. Fracturing holes at LW6305 are all vertical to the roof, and 1# fracturing hole is used to determine the maximum pressure and fracture radius. In 2# and 3# holes twice fracturing at different depth are carried out, respectively.

LW5307 is 210 m wide at beginning and tuned to 125 m because of the fault, and the workplace is about 100 m far away from the corner when we plan to implement the roof fracturing. Micro-seismic results show that mining tremors on the side of the head-entry are much more frequent than the other side, so from the corner and 50 m to the front, roof fracturing must be adopted. And different from LW6305, an inclined hole is also included at LW5307. Fig. 9 indicates the layout of boreholes.

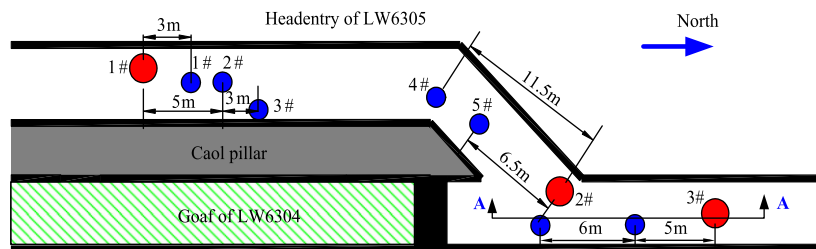
The fracturing boreholes, with diameter 46–48 mm and depth 10–20 m, were pre-drilled into the roadway roof by geological drill-

ing rig. Monitoring drills, used for observing the fracturing radius, were arranged 3 m, 5 m, 7 m, etc. away from the fracturing holes.

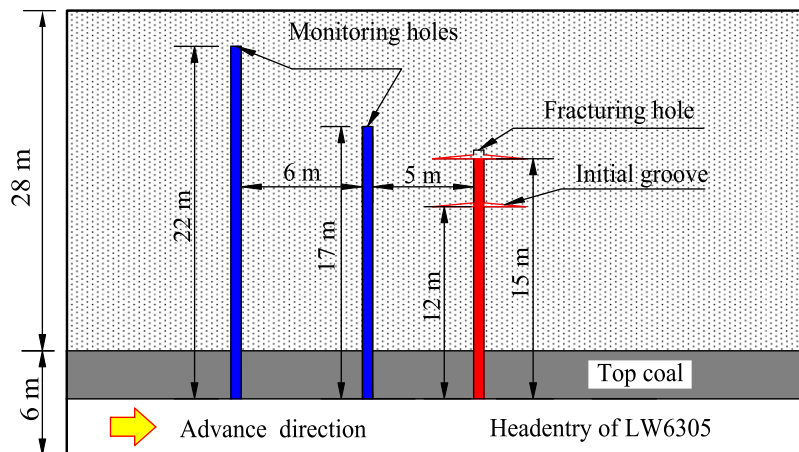
3.2.2. Process of hydraulic fracturing

After monitoring and fracturing boreholes were completed, a special cutting machine, as shown in Fig. 10a, was delivered to the bottom as the aiguille to notch a sharp wedge-shaped initial groove, the quality of the groove is critical for the success of roof fracturing and crack propagating. So, after grooving the detecting must be executed using the strata borescope into the fracturing holes. Fig. 10b shows the failing groove, and this situation must re-groove again, until the shape shown as Fig. 10c which shows a successful cut at the bottom.

The Bimbar-4 seals were selected for borehole sealing, which can afford the maximum liquid pressure of 40 MPa that can fulfill their tasks perfectly. These heads of seals are equipped with a ball valve with a spring. Till the moment when the fracturing pressure exceeds the boundary value of opening of the release valve, the spring presses down the ball to the outlet of the head making the liquid's outflow. The Bimbar-4 was connected with the high pressure hose and lifted into the fracturing holes by manual labor, so the depth was limited within 10 m since the friction and dead weight increased rapidly and restricted the efficiency severely. In order to solve this problem we utilize seamless steel tube to replace the hose as the pipe for high pressure liquid. The steel tube is 1.5 m length per segment equals to the drill rod and special high pressure seals between every two segment, hence geological drill or other similar machines with cohesion and propulsion device can convey the seamless steel tube into the hole automatically to the design depth without any limitation. The efficiency and safety of this experiment greatly improved as automate all the procedures also the steel tube held tightly in case of been thrown out under high pressure liquid.

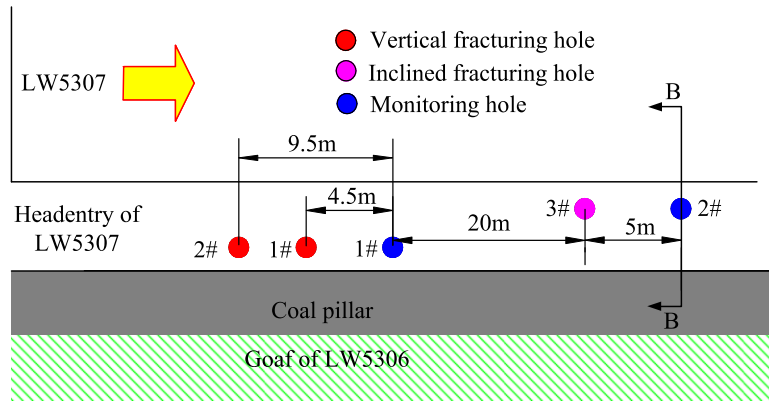


(a) Planar graph of drilling holes layout at LW6305

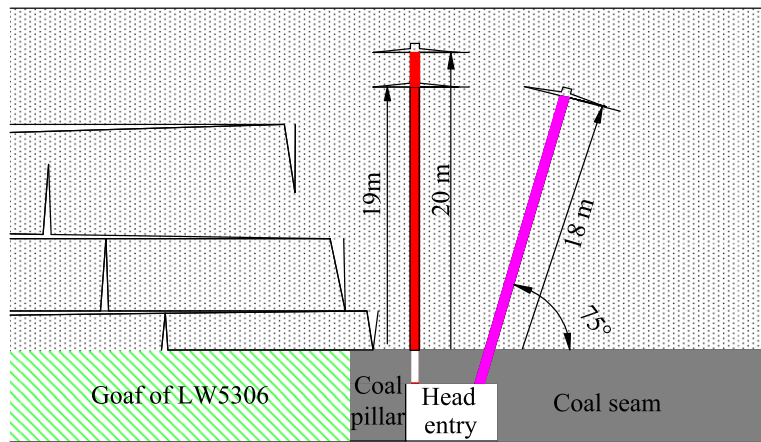


(b) A-A profile of drilling holes layout

Fig. 8. Layout of directional hydraulic fracturing holes at LW6305.



(a) Planar graph of drilling holes layout at LW5307

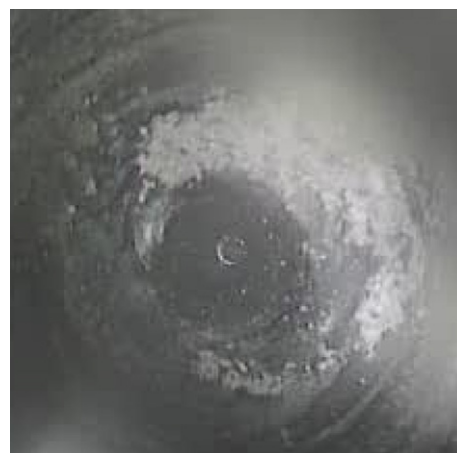


(b) B-B profile of drilling holes layout

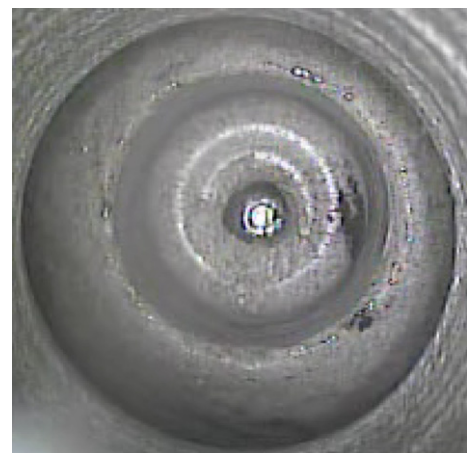
Fig. 9. Layout of directional hydraulic fracturing holes at LW5307.



(a) Initial groove cutting machine



(b) Failing initial groove



(c) Successful initial groove

Fig. 10. Diagram of the cutting machine and initial groove.

3.3. Pressure variation during fracturing

The fracturing process and pressure changes were similar at LW6305 and LW5307, so take 1# fracturing hole at LW6305 as rep-

resentative to describe the phenomena and regularity during the directional fracturing. When fracturing hole was injected with high-pressure emulsion, faint rock rupture sound arose from the close to the distant. About 1 min later, emulsion outflow was ob-

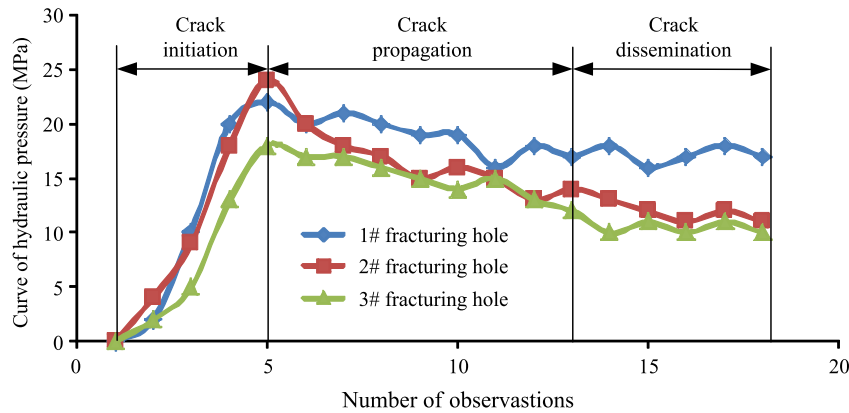


Fig. 11. Graph of pressure variation trend during directional fracturing.

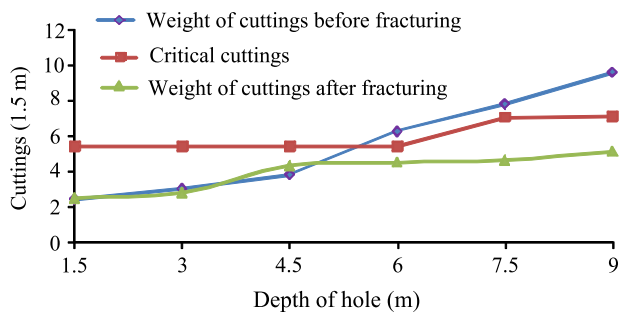


Fig. 12. Drilling cuts variation trend before and after fracturing.

served from monitoring 1# drilling hole, 3 m away from fracturing hole, and the flux grew from small to large, till like raining. 3 min later, emulsion outflow was also observed from 2# monitoring hole that 5 m away from fracturing hole, the flow was significantly less than that from 1# observation drilling, which indicates the propagation rate and radius reduced as decreasing of the flow. The 2# fracturing process at LW6305 also verified the positive relationship between liquid flow and crack propagation velocity and radius, as Fig. 9 showed 5# monitoring hole was 6.5 m far away from 2# fracturing hole, but only 1.5 min after the high pressure liquid injected, the crack plane spread to 5# monitoring hole. During the procedure, digital and direct explicit pressure gauges were used to record the pressure variations. Fig. 11 indicates the pressure changed of three fracturing at LW6305 (the data in this figure were obtained once every 10 s). Similar trends are obviously unfolded that can be divided into three stages. The first stage is pressure from zero to the maximum characterized by increasing rapidly to the required criterion stress P_0 as Eq. (5). The rock mass of the initial groove tip is ruptured after 50 s. Stage two is the crack development to the surroundings, and liquid pressure decline linearly lasted for 2 min and finished at 150 s. Afterwards the third stage the pressure becomes steady which means the fracture plane propagation steady and is approaching to the farthest monitoring hole with fluctuation at 11 MPa.

3.4. Effect verification of rockburst hazard reduction

3.4.1. Test drilling for stress detecting in coal seam

Test drilling method was implemented in order to verify the pressure relief effect of hydraulic fracturing on coal seam. Researches show that coal powders exhausted during the drilling have a positive correlation with stress that if the amount of drilling cuts (coal powder) exceeded the critical index indicates the stress

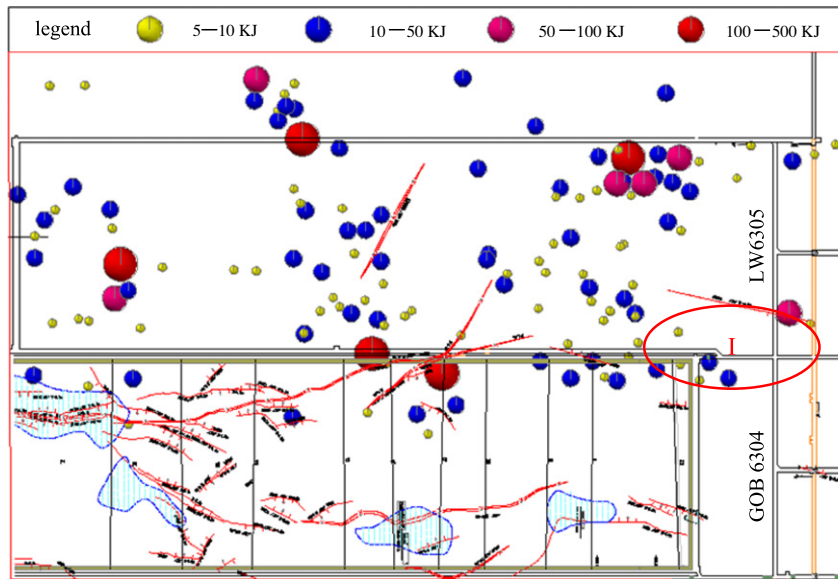
in this area is quite high. Based on this relationship test drilling for rockburst control means testing if a high stress zone exists and, if so, where this zone begins and if it produces borehole bursts or coal rock dynamic effect like drill sucking, sticking, etc., in the drilling process, in the latter case the tendency of the coal to burst under the local stress is also tested. We carried out testing drilling near 1# fracturing hole before roof fractured, as shown in Fig. 12, the drilling cuttings began to exceed the critical cuttings suggested high stress area was found. And after hydraulic fracturing was put into effect, the method was utilized again in this area and drilling cuts was under the critical index within 9 m, also no dynamic effect was encountered, which indicated that hydraulic fracturing to the main roof impair the local stress and greatly diminish impact load, effectively preventing the occurrence of rockburst.

3.4.2. Microseismic system for mining tremors monitoring

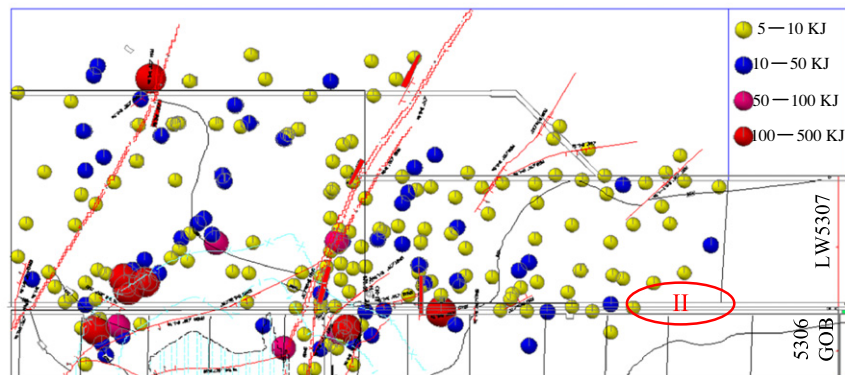
The Seismological Observation System called “SOS” for short with 16 channels that newly developed by Central Mining Institute of Poland was installed around the longwall workfaces to monitor the mining tremors during the coal mining. As one of the most advanced monitoring equipment at home and abroad, SOS can accurately determine the source parameters such as occurring time, coordinates of tremors with minimum energy of 10^2 J and the horizontal location error less than 20 m, the vertical error 30 m under the optimal configuration of seismological network. Fig. 12a shows the distribution of mining tremors in LW6305. The area I is just the directional fracturing zones, tremors in this area reduced obviously compared with previous period in the same roadway and are rather few compared with the other entry, moreover the total energy of tremors occurred in region I is also small. Fig. 13b shows the tremors in LW5307, and region II is the fracturing zone. The same rules are exhibited as LW6305, both the total number and energy reduced significantly. These proved that directional fracture of main roof not only reduces the tremors frequency but also the released energy, that is, eliminate the rockburst hazard. The success of directional fracturing application in LW6305 is conducive to large-scale promotion of this technology in China coal mines that encounter hard roof rockburst and expected to replace the roof blasting.

4. Conclusions

Hard thick roof is the main factor that induces rockburst in most collieries at home and abroad, traditional methods such as blasting and water injection have limited effect on hazard relief since obvious drawbacks. So directional hydraulic fracturing is put forward to control hard roof by cutting out an initial groove in the bore-



(a) Mining tremors distribution during coal mining of LW6305



(b) Mining tremors distribution during coal mining of LW5307

Fig. 13. Mining tremors distribution during coal mining before and after directional fracturing.

holes then injecting high pressure liquid to break the rock mass and drive the crack propagate into the surroundings with a maximum diameter of more than 13 m in Jining No. 3 coal mine.

The model of initial groove is established based on the fracture mechanics, the stress condition for rock cracking on the tip is worked out. The vertical stress distribution around the initial fracture is simulated by a two-dimensional explicit finite difference program FLAC 5.0. The numerical simulation reveals that the vertical compressive stress concentrate 3 times once the initial fracture formed, however the stress state changed immediately to tensile stress when the high pressure injected into the fracturing hole, and the concentration factor up to 5 times as the cutting edge effect and can easily rupture the rock mass.

The seamless steel tube was used to take place of high pressure hose and conveyed into fracturing holes by geological drill to the designed locations without any limitations, so as to make the whole process of this technology automated and greatly improved the efficiency and security.

The pressure of liquid during fracturing process is divided into three stages: dramatically ascending, descending and pressure leveling-off stage, corresponding to crack initiation, propagation and dissemination process, respectively.

In the fractured regions, drilling bits method and microseismic system were used to monitor the stress of coal mass and mining

induced tremors. Both drill cuttings and tremor frequency as well released energy in areas decreased considerably suggests directional fracturing of hard main roof can reduce abutment pressure and rockburst hazard notably thereby confirming the prevention effect of hydraulic directional fracturing.

Acknowledgements

Financial support for this work, provided by the National Basic Research Program of China, (2010CB226805), the National Natural Science Foundation of China (50474068, 50490273), the Independent Foundation of State Key Laboratory of Coal Resources and Safe Mining (SKLCSRSM10X05) and Projects (PAPD) supported by the Priority Academic Program Development of Jiangsu Higher Education Institutions are gratefully acknowledged.

References

- Atkinson, B.K., 1987. Fracture Mechanics of Rock. Academic Press, London.
- Beach, A., 1980. Numerical models of hydraulic fracturing and the interpretation of syntectonic veins. *J. Struct. Geol.* 2, 425–438.
- Bear, J., 1972. Dynamics of Fluids in Porous Media. American Elsevier Publishing Co., Inc., New York.
- Blake, W., Hedley, D.G.F., 2001. Rockbursts: Case Studies from North American Hard-Rock Mines, vol. 41. Society for Mining, Metallurgy, and Exploration, Inc., Littleton, CO., pp. 86–88.

- Board, M., Rorke, T., Williams, G., Gay, N., 1992. Fluid injection for rockburst control in deep mining. In: Balkema, A.A. (Ed.), Proc. 33rd US Symposium on Rock Mechanics, Publ. Rotterdam, Santa Fe, pp. 111–120.
- Brady, B.T., Rowell, G.A., 1986. Laboratory investigation of the electrodynamic of rock fracture. *Nature* 321, 488–492.
- Cook, N.G.W., 1965. A note on rockburst considered as a problem of stability. *J. South Afr. Inst. Min. Metall.* 65, 437–446.
- Dou, L.M., He, X.Q., 2001. Electromagnetic emissions in rock and coal burst failures. *J. Tsinghua Univ.* 41, 86–88.
- Dou, L.M., Zhao, C.G., Yang, S.G., Wu, X.R., 2006. Prevention and Control of Rock Burst in Coal Mine. China University of Mining and Technology Press, Xuzhou.
- Dou, L.M., Lu, C.P., Mu, Z.L., Gao, M.S., 2009. Prevention and forecasting of rock burst hazards in coal mines. *Min. Sci. Technol.* 19, 585–591.
- Du, T.T., Dou, L.M., Yang, J.W., Lu, C.P., He, H., Jiang, H., 2010. Application of rock directional hydraulic fracture. *Coal Min. Technol.* 15, 4–7.
- Dubinski, J.A., 1994. Geophysical assessment of the hydraulic injection process in coal seams under rockburst hazard. In: Rakowski, Z. (Ed.), *Geomechanics 93*. Proc. Conference, Ostrava, pp 55–58.
- Fairhurst, C., 1964. Measurement of in-situ rock stresses with particular reference to hydraulic fracturing. *Rock Mech. Eng.* 2, 129–134.
- Fujii, Y., Ishijima, Y., Deguchi, G., 1997. Prediction of coal face rockbursts and microseismicity in deep longwall coal mining. *Int. J. Rock Mech. Min. Sci.* 34, 85–96.
- García, J.E.L., Sousa, J.L.A.O., 1997. A quasi-analytical model for three-dimensional analysis of hydraulic fracture propagation in reservoir rocks. *Int. J. Rock Mech. Min. Sci.* 34 (297), e1–e15.
- Gibowicz, S.J., Kijko, A., 1994. *An Introduction to Mining Seismology*. Academic Press, San Diego.
- Haimson, B., Fairhurst, C., 1970. In situ stress determination at great depth by means of hydraulic fracturing. In: Somerton, W.H. (Ed.), Proc. 11th US Rock Mech. Symp., Am. Inst. Min. Eng., New York, pp. 559–584.
- He, M.C., Nie, W., Han, L.Q., Ling, L.J., 2010. Microcrack analysis of Sanya granite fragments from rockburst tests. *Min. Sci. Technol.* 20, 238–243.
- Huang, B.X., Deng, G.Z., Liu, C.Y., 2007. Hydraulic fracturing weakening technology of coal and rock mass and its progress. *Eng. Sci.* 9, 83–88.
- Ito, T., Evans, K., Kawai, K., Hayashi, K., 1999. Hydraulic fracture reopening pressure and the estimation of maximum horizontal stress. *Int. J. Rock Mech. Min. Sci.* 36, 811–826.
- Klishin, S.V., 2006. Destruction of rocks by directional hydraulic fracturing on the basis of models of plasticity with internal variables. In: Mota Soares, C.A., et al. (Eds.), III European Conference on Computational Mechanics Solids, Structures and Coupled Problems in Engineering. Lisbon, Portuga. pp. 25.
- Lenoach, B., 1995. The crack tip solution for hydraulic fracturing in a permeable solid. *J. Mech. Phys. Solids* 43, 1025–1043.
- Li, T., Cai, M.F., Cai, M., 2007. A review of mining-induced seismicity in China. *Int. J. Rock Mech. Min. Sci.* 44, 1149–1171.
- Mansurov, V.A., 2001. Prediction of rockbursts by analysis of induced seismicity data. *Int. J. Rock Mech. Min. Sci.* 38, 893–901.
- Mofazzal, H.M.D., Rahman, M.K., 2008. Numerical simulation of complex fracture growth during tight reservoir stimulation by hydraulic fracturing. *J. Petrol. Sci. Eng.* 60, 86–104.
- Papanastasiou, P.C., 1997. A coupled elastoplastic hydraulic fracturing model. *Int. J. Rock Mech. Min. Sci.* 34, 240–254.
- Rahman, M.K., Joarder, A.H., 2006. Investigating production-induced stress change at fracture tips: implications for a novel hydraulic fracturing technique. *J. Petrol. Sci. Eng.* 51, 185–196.
- Ruiting, W., 2006. Some fundamental mechanisms of hydraulic fracturing. Ph.D. Thesis, Georgia Institute of Technology, Atlanta.
- Salamon, M.D.G., 1984. Energy considerations in rock mechanics: fundamental results. *J. South Afr. Inst. Min. Metall.* 84, 233–246.
- Sharan, S.K., 2007. A finite element perturbation method for the prediction of rockburst. *Comput. Struct.* 85, 1304–1309.
- Srinivasan, C., Arora, S.K., Yaji, P.K., 1997. Use of mining and seismological parameters as premonitors of rockbursts. *Int. J. Rock Mech. Min. Sci.* 34, 1001–1008.
- Tang, B.Y., 2000. Rockburst control using destress blasting. Ph.D. Thesis, McGill University.
- Wang, Z.T., Zhou, H.Q., Xie, Y.S., 2008. *Mining Rock Mass Mechanics*. China University of Mining and Technology Press, Xuzhou.
- Yan, S.H., Ning, Y., Kang, L.J., Shi, Y.W., Wang, Y.G., Li, Y.F., 2000. The mechanism of hydrobreakage to control hard roof and its test study. *J. China Coal Soc.* 25, 32–35.
- Zhu, W.C., Li, Z.H., Zhu, L., Tang, C.A., 2010. Numerical simulation on rockburst of underground opening triggered by dynamic disturbance. *Tunn. Undergr. Space Technol.* 25, 587–599.